ACS APPLIED NANO MATERIALS

www.acsanm.org Article

Carbon Quantum Dots as Fluorescence Nanochemosensors for Selective Detection of Amino Acids

Nunzio Tuccitto,* Luca Fichera, Roberta Ruffino, Valentina Cantaro, Gianfranco Sfuncia, Giuseppe Nicotra, Giuseppe Trusso Sfrazzetto, Giovanni Li-Destri, Andrea Valenti, Antonino Licciardello, and Alberto Torrisi

Cite This: https://doi.org/10.1021/acsanm.1c01046 Read Online

ACCESS | Metrics & More | Article Recommendations | Supporting Information

ABSTRACT: Fluorescent carbon quantum dots (CDs) are synthesized and employed as fluorescent nanochemosensors for selective detection of amino acids. A detailed investigation of excitation−emission maps revealed that the fluorescence properties of CDs are intensely and strongly influenced by the interaction at the surface with different amino acids. The discrimination capability was demonstrated by tensor rank decomposition of the differences induced by the surface reaction in the excitation−emission maps and by means of a common machine learning approach based on artificial neural networks.

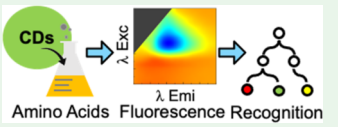

KEYWORDS: *nanoparticles, amino acids, machine learning, sensors, chemospecific*

INTRODUCTION

Carbon quantum dots (CDs) are carbon nanoparticles smaller than 10 nm having attractive photoluminescence properties, good water solubility, high stability, and biocompatibility. The name derives from the most important property that characterizes them: fluorescence, which allows them to be assimilated to quantum dots, nanoparticles of fluorescent semiconductors. They differ from these because they are mainly composed of carbon, a generally nontoxic element, which is expected to represent a significant advantage for their application in the biological field. The name CDs, therefore, reflects the composition and property of emitting light at different wavelengths from the incident. Since their discovery by Xu et al. in 2004,[1] CDs have been applied for different basic research circumstances and very technical applications ranging from molecular communication[2−5] to theranostics,[6] as well as for the detection of specific analytes[7,8] with particular reference to metal ions.[9−11] Moreover, as demonstrated by Sun et al., CD fluorescence yield is greatly increased through surface passivation.[12] Although the chemical−physical mechanism underlying CD fluorescence is not yet fully understood,[13] it is found in the literature that fluorescence can be modulated through several factors: particle size (quantum effect), surface groups, surface defects, and fluorophores with different degrees of π conjugation and electron holes located between the sp^2 carbons of the clusters and the sp^3 carbons of the matrices.[14−16] Recent studies have shown that the optical properties vary considerably depending on the synthesis methodology used, passivation, doping, and size of the CDs.[17−22] This suggests that fluorescence may depend on the surface of the nanoparticles, in particular on the "surface defects" that may be responsible for absorption at certain wavelengths.[23] Therefore, the functionalization of the surface of CDs can change the fluorescence characteristics in terms of emission intensity and excitation and emission wavelengths. This makes CDs suitable for the detection of natural molecules. In particular, CDs are synthesized by hydrothermal decomposition that produces at their surface hydroxy, carbonyl, carboxylic, ether, and epoxy groups, and these nanoparticles are suitable for reaction with amine groups.[24] The capability of selective identification of amino acids is central to the diagnosis of various conditions including neural degenerative diseases,[25] spina bifida,[26] metabolic disorders,[27] and so on. Several methods were reported for amino acid determination.[28] Gao et al. proposed an array for natural amino acid sensing based on the interaction between CDs and metal ions.[29] However, such methods suffer from complex sample pretreatment or low sensitivity. What we propose to overcome these limitations is a chemosensor strategy, shown in Scheme 1, through the combined use of bare CDs and the application of multivariate analysis and fluorescent nanochemosensors.

Using the standard EDC/NHS approach (EDC: (1-ethyl-3-(−3-dimethylaminopropyl)carbodiimide hydrochloride and NHS: N-hydroxy succinimide),[30] we activated the carboxyl groups on nanoparticle surfaces and then made them react with different amino acids. The detailed study of the obtained fluorescence spectra allowed us not only to recognize each

Received: April 16, 2021
Accepted: May 18, 2021

Scheme 1. Pictorial Representation of Amino Acid Recognition Based on the Effect on the CD Fluorescence Coupled with Machine Learning Capabilities

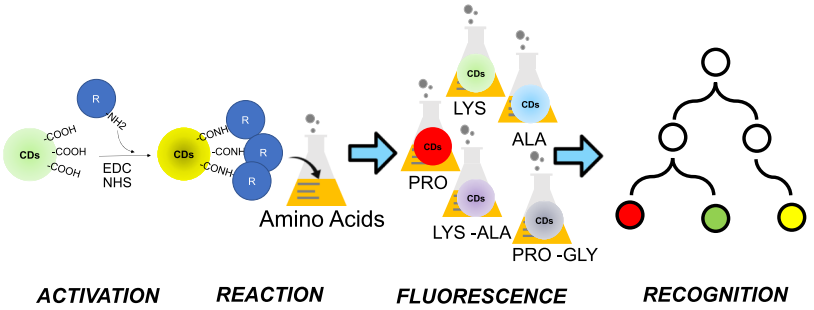

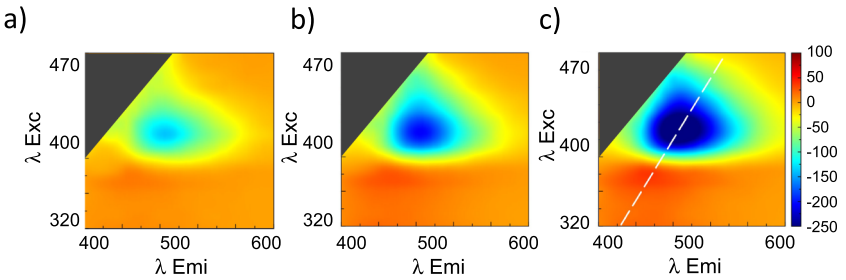

Figure 1. Map of fluorescence difference after surface functionalization of activated CDs with GLY at various concentrations: (a) 0.5, (b) 1.0, and (c) 1.5 μg/mL

amino acid upon reaction with nanoparticles, but also to discriminate among them in a mixture of amino acids in which these nanochemosensors were previously immersed.

MATERIALS AND METHODS

CDs were synthesized by hydrothermal decomposition of citric acid (from Aldrich Milan, Italy). In a typical procedure of CD synthesis, 7 g of citric acid were put into a 20 mL beaker and heated at 205 °C. About 10 min later, salts were liquefied obtaining a pale-yellow liquid, which turned dark green in 15 min, implying the formation of CDs. The obtained brown liquid was cooled down to room temperature, and 50 mL of 0.25 M aqueous solution of NaOH (Aldrich, Milan, Italy) was added dropwise under vigorous stirring. The solution was centrifuged at 6000 RPM for 5 min, and the supernatant solution was dialyzed for 24 h using a tube having 11′000 Da cutoff (Aldrich, Milan, Italy). Water was evaporated using a rotary evaporator under vacuum at 40 °C to obtain dry CDs. From 7 g of starting raw material, typically around 200 mg of dry CDs was collected. The fluorescence efficiency of the CDs was evaluated according to ref 31. The as-prepared CDs presented 11% efficiency. The amino acid solutions glycine (GLY), alanine (ALA), proline (PRO), aspartic acid (ASP), lysine (LYS), and histidine (HYS) (from Aldrich Milano, Italy) were prepared in phosphate buffer at pH 7.4 (from Aldrich Milano, Italy). Activation with EDC (1-ethyl-3-(−3-dimethylaminopropyl)-carbodiimide hydrochloride, from Aldrich Milano, Italy) and NHS (N-hydroxy succinimide, from Aldrich Milano, Italy) was performed according to ref 30. The activation reaction was performed at room temperature. Fluorescence characterization was performed using a Cary Eclipse instrument (Agilent). The fluorescence characterization was performed within 30 min. It was verified that within this time range the difference maps did not vary significantly (vide infra). Fourier-transform infrared spectroscopy (FT-IR) characterization was performed in KBr tablets of dried nanoparticles with a Spectrum Two instrument (PerkinElmer). Atomic force microscopy (AFM) characterization was performed with a Nanoscope IIIA instrument (Veeco). The transmission electron microscopy (TEM) analysis was performed in a conventional bright-field configuration with a JEOL ARM200F operated at 200KeV and equipped with a Gatan Image Filter (GIF) and a Gatan UltraScan 1000XP (2 k × 2 k) charge-coupled device camera. Images were obtained filtering only the elastic scattering component of the transmitted electron beam and at a low electron dose to increase the contrast and to reduce the beam damage, respectively. The TEM sample was prepared by drop casting the nanoparticle dispersion on an ultrathin (<3 nm) carbon film TEM grid. More than 650 CDs were detected and measured. The size distribution, fitted with a Gaussian, gave a measure of 14.1 ± 5.8 nm of the diameter. Data processing including the analysis of the principal components and machine learning were performed by means of Python scripts developed in house using the Numpy, SciPy, and Matplotlib libraries.

RESULTS AND DISCUSSION

The size and morphology of CDs were determined by AFM and TEM (see Figure S1). Both indicate that the formed CDs were mainly spherical in shape, with the diameter in a range of 10 nm, as revealed by section analysis. X-ray diffraction (XRD) measurements (see Figure S2) revealed that CDs have a single broad diffraction peak centered around 25°, which is attributed to the (002) lattice spacing of carbon-based materials with amorphous nature. CDs show optical absorption mainly in the ultraviolet region with a strong absorption band below 300 nm, which is attributed to the $\pi-\pi^*$ transition of the aromatic C═C units located at the nanoparticle core, and a weak band shoulder above 330 nm assigned to the $n-\pi^*$ transition corresponding to the carbonyl functional groups on the surface (see Figure S3a). Further confirmation of surface functional groups of CDs was obtained from FT-IR spectra. The typical spectrum is reported in Figure S3b, which exhibits a broad peak around ∼3400 cm^{-1} corresponding to the O−H stretching attributed to hydroxylic groups, and displays the C−H stretching zone with a maximum at ∼2920 cm^{-1}, and the C═C aromatic stretching at ∼1650 cm^{-1} shows a peak at 1721 cm^{-1} assigned to the stretching of C═O (related to carbonyl). All of these suggest that the carboxylic functional groups are present on the surface of CDs. The observation of the CD fluorescence spectra shows, as expected, a dependence

https://doi.org/10.1021/acsanm.1c01046
ACS Appl. Nano Mater. XXXX, XXX, XXX−XXX

of both fluorescence maximum and intensity on the excitation wavelength. Figure S4a shows the fluorescence map (nominally excitation−emission) in false colors of CDs synthesized by hydrothermal decomposition. Light colors mean high emission while dark colors mean low fluorescence intensity. CDs show a fluorescence maximum at 490 nm when excited around 410 nm. Upon interaction with an amino acid, carboxyl groups (activated with the standard method concerning EDC/NHS[30]) are expected to react with the amino group by changing the physical chemical nature of the surface, hence affecting the fluorescence (Figure S4b). At this concentration, GLY does not show remarkable fluorescence properties in the range of the wavelengths explored in comparison with CD emission. To reveal the change of fluorescence induced by the reaction with the amino acid, we made maps obtained as the difference between those of excitation−emission of activated CDs after reaction with GLY at different concentrations (ranging from 0.5 to 1.5 μg/mL) and the one of the as-prepared CDs. These maps are shown in Figure 1, indicating with warm colors an increase of fluorescence compared to naked CDs, while with cold colors a decrease of fluorescence, as a result of functionalization. The effect is clear and indisputable; indeed, the increase of the GLY concentration causes a strong increase in the observed fluorescence. It suggests that the effect observed on the activated CDs is not due to a simple contact but due to a chemical reaction between the amino acid groups of GLY and carboxyl groups present at the CD surface. Conversely, the difference maps obtained for nonactivated CDs in the presence of GLY appear merely noisy (Figure S5a) with low intensity, indicating that no reaction occurred and that, at least at the GLY concentration used (10 μg/mL) the effect of amino acids on the CD fluorescence is not detectable. Consequently, the activation is a "sine qua non" step.

It might suggest that the effect that we are observing when CDs are activated is due to the interaction between the amino acid groups of amino acids and carboxyl groups present on the surface of CDs that when not activated do not affect the fluorescence because they do not react.

Figure 2a shows that the variation of the fluorescence obtained from the section analysis of fluorescence difference maps obtained analyzing several GLY solutions upon reaction with CDs calculated along the white dotted line as shown in Figure 1c. The plot of the peak-valley distance ($\boldsymbol{\Delta I}$) reported in Figure 2b as a function of concentration clearly shows a saturation trend. The data were fitted with the Langmuir model governing the adsorption. Figure 2c reports a plot like that shown in Figure 2b but obtained at lower concentrations. To allow easier quantitative evaluation, for the sake of simplicity, one can assume a direct proportionality between ΔI and GLY concentration. Several replicas in this range led to estimation of a $\boldsymbol{\Delta I}$ uncertainty of ±10 (a.u.). Therefore, we assume a minimum detectability limit of about 0.1−0.2 μg/mL, although more accurate evaluations are necessary if a rigorous analytical method would be developed. Because the amide bond is expected to be reversible,[32] we explored whether the fluorescence of CDs would change with time after prolonged immersion in GLY solutions at different concentrations. Figure 2d shows the plot of the variation of fluorescence intensity as a function of time. The trend is complex, depending on the concentration. At high concentrations, the decrease appears to be linear, while at concentrations lower than 2 μg/mL the initial linear decrease is followed by an exponential decay, which leads, at long times

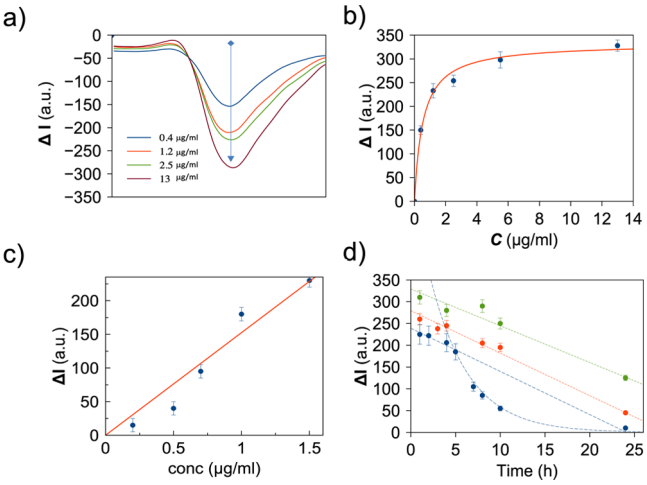

Figure 2. (a) Fluorescence intensity acquired by the section analysis along the white dotted line drawn in Figure1c. (b) Variation of fluorescence intensity as a function of GLY concentration; the red line is the plot of the best fit of data by the Langmuir model for the concentration above 1.5 μg/mL and in (c) is the linear best fit of data related to low concentration of GLY (below 1.5 μg/mL). (d) Variation of fluorescence intensity as a function of time. Dotted lines are drawn to help the reader's eye.

(overnight) a reduction of the fluorescence of the functionalized CDs to that measured in the as-prepared CDs. Similar results have been obtained with different amino acids. Also, ALA, PRO, ASP, LYS, and HYS were selected. The determination of these analytes could have important repercussions in biomedical applications. For example, in cystinuria there is increased excretion of lysine in urine, which results in kidney stones.[33] The rare metabolic condition known as Prolidase deficiency could benefit from the prompt determination of proline.[34] Liver damage could result in pathologic alanine aminotransferase behavior causing uncontrolled variation of alanine.[35] Histidinemia is an inherited condition characterized by elevated blood levels of the amino acid histidine. Histidinemia typically causes no health problems, and most people with elevated histidine levels are unaware that they have this condition.[35] Because time-of-flight secondary ion mass spectrometry (ToF-SIMS) is a surface-sensitive mass spectrometry technique, it is possible to verify that amino acid-related fragments are detected on the surface of CDs after purification, based on dialysis, which confirms the anchoring reaction. Figure S6 shows an extract of the characterization of ToF-SIMS, for the sake of brevity. These results may suggest that by varying the chemical nature of the group that chemically bonds to the surface, a different, selective, chemospecific effect on the fluorescence of CDs could emerge. To carry out an evaluation of the effect of the reaction of carboxyl groups on the fluorescence properties of CDs, we have carried out an extensive analysis program acquiring several excitation−emission maps and numerous replicas for various amino acids at 10 μg/mL. At this concentration, none of the analyzed amino acids show remarkable fluorescence properties in the range of the wavelengths explored in comparison with CD emission. The excitation−emission maps of these samples were assembled to make a three-dimensional tensor consisting of 25 excitation wavelength values × 400 emission wavelength values × 60 samples (10 replicas per amino acid) that add up to 6 × 10^5

https://doi.org/10.1021/acsanm.1c01046
ACS Appl. Nano Mater. XXXX, XXX, XXX−XXX

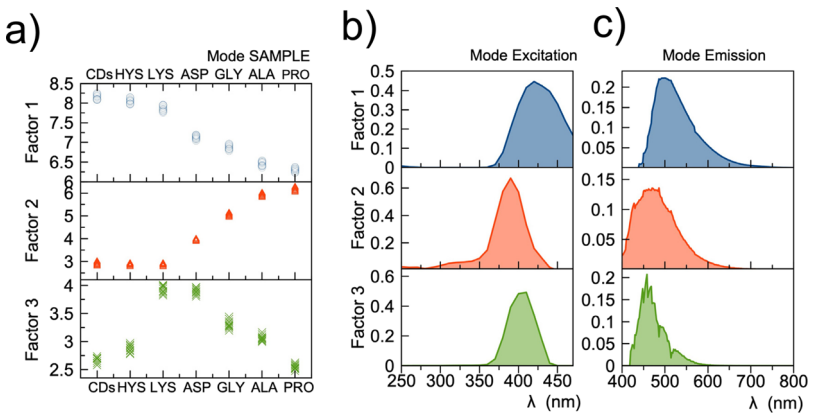

Figure 3. Results of NON-NEGATIVE-PARAFAC decomposition: (a) sample mode, (b) excitation mode, and (c) emission mode. Percentages of variance explained are 78% for Factor 1, 84% up to Factor 2, and 87% up to Factor 3.

values. We applied a method of tensor rank decomposition known as PARAFAC to facilitate data processing and to have an objective and operator-independent evaluation of these results.[36,37] PARAFAC is a generalization of principal component analysis to higher order arrays where, compared to other methods, there is no rotation problem of the matrix, and for example, pure spectra can be recovered from a multiway spectral data tensor. In particular, we have used a NON-NEGATIVE-PARAFAC[38,39] method because the fluorescence and excitation spectra are always positive, and the output of the decomposition will be easier to interpret. We calculated the sum of the residual decomposition as the rank increases, so we have chosen to make a rank-3 decomposition where the residue is minimum. Figure 3 shows the result of the rank 3 decomposition.

The sample mode shows that the differences between the 10 replicas are less relevant than the differences between the several amino acids under investigation, paving the way for the possibility of using CDs as nanosensors sensitive to different amino acids. It is not easy to assign the physicochemical meaning to factors obtained by the PARAFAC analysis. In the literature, it has been reported that factors may be related to the property of the different substances, to the concentration of the analytes, or to some other characteristic not easily identifiable.[39] In the case under investigation, it is possible to find a direct correlation between the hydrophobic or hydrophilic properties of the lateral groups of the amino acids and the values of the first and second factors, respectively. The third factor discriminates LYS and ASP, which are two of the amino acids with the most relevant electrical charge in the lateral group, among those investigated.

Figure 4 shows the representation of the mode of the samples in the three-dimensional space consisting of the three factors. The plot shows that the individual amino acids are discriminated without significant overlapping between the clusters of the replicates. These results confirm that by analyzing a large data set with an unsupervised data treatment method the variations of the replicates are lower than the differences between the different samples. Thus, CDs could be used as nanochemosensors for discriminating amino acids at concentrations in the order of 10 μg/mL. The analysis of the excitation and emission mode confirms that the discrimination is obtained thanks to variations in the excitation and emission properties of CDs.

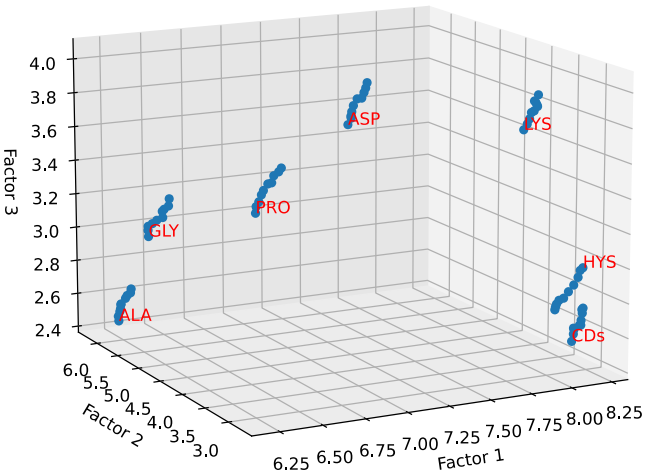

Figure 4. 3D representation of the first three factors of NON_-NEGATIVE PARAFAC decomposition. Dots represent sample replicas. Red labels show the amino acid used for surface functionalization of activated CDs.

For more insight, Figure 5 shows the effect of different amino acids on the fluorescence variation of activated CDs. The variation is significant between different amino acids at the concentration needed to reach the saturation region (10 μg/mL). A closer investigation confirms a correlation between the chemical nature of the amino acid and the effect on the variation of the excitation−emission map. Note, for example, the similarity of the effect of GLY, ALA, and PRO compared to the others. Certainly, they are chemically more similar to each other when compared to the other amino acids investigated as, for example, GLY and ALA only differ for one methyl group. The effect on the variation of the excitation−emission map is still clearly discernible but is very similar. If, by comparison, the effect of ASP is observed, the chemical difference in the lateral group is reflected on a significant variation of the fluorescence of CDs, because of interaction with the amino acid. In particular, amino acids having higher hydrophilic features affect the excitation of CDs around 425 nm and the emission around 500 nm, decreasing the intensity of the emission compared to naked CDs (please refer to Figure 5a−c). The hydrophobic group is characterized by an effect on the excitation around 380 nm and the emission at 470 nm, increasing fluorescence compared to naked CDs (please refer to Figure 5d-f).

https://doi.org/10.1021/acsanm.1c01046
ACS Appl. Nano Mater. XXXX, XXX, XXX−XXX

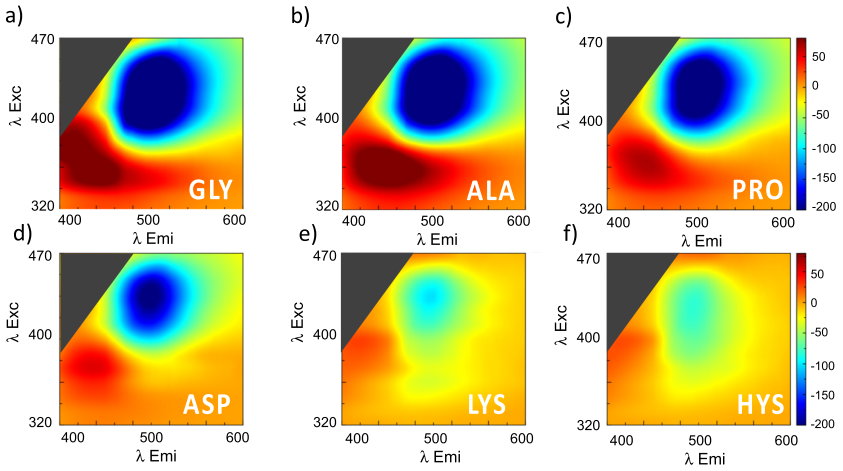

Figure 5. Fluorescence variation maps of activated CDs after reaction with several amino acids (10 μg/mL) as labeled in the pictures, (a) GLY, (b) ALA, (c) PRO, (d) ASP, (e) LYS, and (f) HYS.

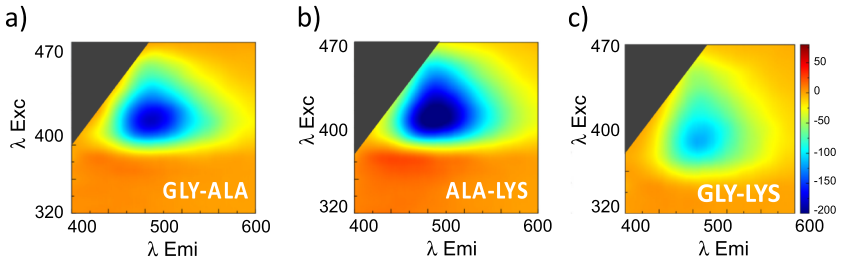

Figure 6. Fluorescence variation maps of activated CDs after reaction with several equimolar mixtures of amino acids (10 μg/mL) as labeled in the pictures, (a) GLY mixed with ALA, (b) ALA mixed with LYS, and (c) GLY mixed with LYS.

Table 1. Confusion Matrix

	predicted ALA	predicted not-ALA	
actual ALA	TRUE POSITIVE (TP) 8	FALSE NEGATIVE (FN) 2	sensitivity: TP/(TP + FN) = 0.80
actual not-ALA	FALSE POSITIVE (FP) 7	TRUE NEGATIVE (TN) 73	specificity TN/(FP + TN) = 0.91

Figure 6 shows the effect on fluorescence of the binary mixture of three amino acids. CDs reacted with equimolar mixtures of GLY-ALA, ALA-LYS, and GLY-LYS. The observed modification of the CD excitation−emission maps with respect to the ones obtained using a single amino acid shows that this effect is not merely additive. In particular, the three binary maps are distinguishable with respect to that obtained using single amino acid solutions, and in addition they are distinguishable from each other. This implies that the shell of mixed amino acids anchored on the surface of the CDs will have a unique and distinguishable effect opening the way to a variety of applications, like the potential application of CDs as fluorescent probes sensitive to discrimination of complex mixtures. To provide an example of the potential application of CDs as nanosensors for selective recognition of amino acids we have trained an artificial neural network for ALA recognition among other amino acids including mixtures. The performance of the classification of the algorithm is summarized in Table 1 by means of the confusion matrix.

Each row of the matrix corresponds to a predicted class; in this case, the output is binary ALA or not ALA. Similarly, each column of the matrix corresponds to any actual class. The counts of correct and incorrect classification are then filled into the table. The total number of correct predictions for ALA goes into the expected row for the ALA class value and the predicted column for that class value. In the same way, the total number of incorrect predictions for a class goes into the expected row for that class value and the predicted column for that class value. In particular, values within the confusion matrix are the average percentage of entries within that cell. It seems evident that our results confirm the proposed application with valuable sensitivity and specificity. Further studies and optimization of the machine learning process and anti-interference experiments would be necessary but have not been performed because it would be a mere exercise that goes beyond the scope of our study.

CONCLUSIONS

This study showed encouraging results on the application of CDs as fluorescent nanochemosensors. A careful analysis of the excitation−emission maps proved that the fluorescence properties of EDC/NHS activated CDs have potential applications in the analytical field of the selective recognition of various chemical compounds. In particular, we demonstrated that EDC/NHS activated CDs show dramatic differences in their fluorescence properties when bound to different amino acids. This effect, which easily allows discriminating hydrophobic amino acids from polar ones, can be further refined to selectively recognize single amino acids even when mixed with other ones. We believe that our findings will help

https://doi.org/10.1021/acsanm.1c01046
ACS Appl. Nano Mater. XXXX, XXX, XXX−XXX

the development of novel and inexpensive nanochemosensors for both the investigation of specific diseases, which are currently diagnosed by simple amino acid detection, including in the framework of bioimaging and for the quality control of food and beverage, whose putrefaction is accompanied by the biosynthesis of characteristic amine.

■ ASSOCIATED CONTENT

Supporting Information

The Supporting Information is available free of charge at https://pubs.acs.org/doi/10.1021/acsanm.1c01046.

Additional supporting figures regarding AFM, TEM, UV−vis, FT-IR, XRD, ToF-SIMS, and fluorescence characterization. Python-based script developed for data treatment is reported (pdf)

■ AUTHOR INFORMATION

Corresponding Author

Nunzio Tuccitto − *Laboratory for Molecular Surfaces and Nanotechnology-CSGI, 95125 Catania, Italy; Department of Chemical Sciences, Università degli Studi di Catania, 95125 Catania, Italy;* orcid.org/0000-0003-4129-0406; Email: nunzio.tuccitto@unict.it

Authors

Luca Fichera − *Department of Chemical Sciences, Università degli Studi di Catania, 95125 Catania, Italy;* orcid.org/0000-0002-7150-7744

Roberta Ruffino − *Department of Chemical Sciences, Università degli Studi di Catania, 95125 Catania, Italy;* orcid.org/0000-0002-9460-925X

Valentina Cantaro − *Laboratory for Molecular Surfaces and Nanotechnology-CSGI, 95125 Catania, Italy;* orcid.org/0000-0002-8809-4886

Gianfranco Sfuncia − *Consiglio Nazionale delle Ricerche, Istituto per la Microelettronica e Microsistemi, Catania I-95121, Italy;* orcid.org/0000-0001-7355-7692

Giuseppe Nicotra − *Consiglio Nazionale delle Ricerche, Istituto per la Microelettronica e Microsistemi, Catania I-95121, Italy*

Giuseppe Trusso Sfrazzetto − *Department of Chemical Sciences, Università degli Studi di Catania, 95125 Catania, Italy;* orcid.org/0000-0003-1584-5869

Giovanni Li-Destri − *Laboratory for Molecular Surfaces and Nanotechnology-CSGI, 95125 Catania, Italy; Department of Chemical Sciences, Università degli Studi di Catania, 95125 Catania, Italy;* orcid.org/0000-0001-6195-659X

Andrea Valenti − *Department of Chemical Sciences, Università degli Studi di Catania, 95125 Catania, Italy;* orcid.org/0000-0001-8645-3331

Antonino Licciardello − *Laboratory for Molecular Surfaces and Nanotechnology-CSGI, 95125 Catania, Italy; Department of Chemical Sciences, Università degli Studi di Catania, 95125 Catania, Italy;* orcid.org/0000-0001-5146-8971

Alberto Torrisi − *Department of Chemical Sciences, Università degli Studi di Catania, 95125 Catania, Italy;* orcid.org/0000-0002-0940-7750

Complete contact information is available at: https://pubs.acs.org/10.1021/acsanm.1c01046

Author Contributions

L.F. performed UV−vis, FT-IR, and fluorescence spectroscopic characterization. He managed the data processing and participated in the writing of the article. R.R. performed AFM and XRD characterization. She managed the data processing and participated in the writing of the article under the supervision of Prof. Giovanni Li-Destri both managed the data processing and participated in the writing of the article. V.C. performed nanoparticle synthesis, activation, and reaction with amino acids under the supervision of Prof. Giuseppe Trusso Sfrazzetto both managed the data processing and participated in the writing of the article. Dr. G.S. performed TEM characterization under the supervision of Dr. G.N. both managed the data processing and participated in the writing of the article. A.V. performed ToF-SIMS characterization under the supervision of Prof. A.L. both managed the data processing and participated in the writing of the article. Prof. N.T. conceptualized and designed the experiments, supervised the experiments, analyzed the data including machine learning, managed the data report, drafted the article, managed the correspondence, and edited the article up to the final version. Prof. A.T. managed the multivariate analysis, supervised the whole workgroup, and finalized the article writing. All authors have given approval to the final version of the manuscript.

Funding

From Italian Ministry of Education and Research to University of Catania for project. NatI4Smart in the framework of Programma ricerca di ateneo UNICT 2020−22 linea 2. From Italian Ministry of Education and Research to CNR-IMM for project Beyond-Nano (PON a3_00363).

Notes

The authors declare no competing financial interest.

■ ACKNOWLEDGMENTS

Nunzio Tuccitto and Alberto Torrisi thanks "Programma ricerca di ateneo UNICT 2020-22 linea 2" Proj. NatI4Smart for funding. Part of this work was performed at Beyondnano CNR-IMM, which is supported by the Italian Ministry of Education and Research (MIUR) under project Beyond-Nano (PON a3_00363).

■ ABBREVIATIONS

GLY, glycine
ALA, alanine
PRO, proline
ASP, aspartic acid
LYS, lysine
HYS, histidine

■ REFERENCES

(1) Xu, X.; Ray, R.; Gu, Y.; Ploehn, H. J.; Gearheart, L.; Raker, K.; Scrivens, W. A. Electrophoretic Analysis and Purification of Fluorescent Single-Walled Carbon Nanotube Fragments. *J. Am. Chem. Soc.* **2004**, *126*, 12736−12737.

(2) Li-Destri, G.; Fichera, L.; Zammataro, A.; Trusso Sfrazzetto, G.; Tuccitto, N. Self-Assembled Carbon Nanoparticles as Messengers for Artificial Chemical Communication. *Nanoscale* **2019**, *11*, 14203−14209.

(3) Tuccitto, N.; Li-Destri, G.; Messina, G. M. L.; Marletta, G. Fluorescent Quantum Dots Make Feasible Long-Range Transmission of Molecular Bits. *J. Phys. Chem. Lett.* **2017**, *8*, 3861−3866.

(4) Fichera, L.; Li-Destri, G.; Ruffino, R.; Messina, G. M. L.; Tuccitto, N. Reactive Nanomessengers for Artificial Chemical Communication. *Phys. Chem. Chem. Phys.* **2019**, *21*, 16223−16229.
(5) Fichera, L.; Li-Destri, G.; Tuccitto, N. Fluorescent Nanoparticle-Based Internet of Things. *Nanoscale* **2020**, *12*, 9817−9823.
(6) Zheng, X. T.; Ananthanarayanan, A.; Luo, K. Q.; Chen, P. Glowing Graphene Quantum Dots and Carbon Dots: Properties, Syntheses, and Biological Applications. *Small* **2015**, *11*, 1620−1636.
(7) Tuccitto, N.; Riela, L.; Zammataro, A.; Spitaleri, L.; Li-Destri, G.; Sfuncia, G.; Nicotra, G.; Pappalardo, A.; Capizzi, G.; Trusso Sfrazzetto, G. Functionalized Carbon Nanoparticle-Based Sensors for Chemical Warfare Agents. *ACS Appl.Nano Mater.* **2020**, *3*, 8182−8191.
(8) Zammataro, A.; Gangemi, C. M. A.; Pappalardo, A.; Toscano, R. M.; Puglisi, R.; Nicotra, G.; Fragalà, M. E.; Tuccitto, N.; Sfrazzetto, G. T. Covalently Functionalized Carbon Nanoparticles with a Chiral Mn-Salen: A New Nanocatalyst for Enantioselective Epoxidation of Alkenes. *Chem. Commun.* **2019**, *55*, 5255−5258.
(9) Gedda, G.; Lee, C. Y.; Lin, Y. C.; Wu, H. F. Green Synthesis of Carbon Dots from Prawn Shells for Highly Selective and Sensitive Detection of Copper Ions. *Sens. Actuators B* **2016**, *224*, 396−403.
(10) Salinas-Castillo, A.; Ariza-Avidad, M.; Pritz, C.; Camprubí-Robles, M.; Fernández, B.; Ruedas-Rama, M. J.; Megia-Fernández, A.; Lapresta-Fernández, A.; Santoyo-Gonzalez, F.; Schrott-Fischer, A.; Capitan-Vallvey, L. F. Carbon Dots for Copper Detection with down and Upconversion Fluorescent Properties as Excitation Sources. *Chem. Commun.* **2013**, *49*, 1103−1105.
(11) Wang, F.; Gu, Z.; Lei, W.; Wang, W.; Xia, X.; Hao, Q. Graphene Quantum Dots as a Fluorescent Sensing Platform for Highly Efficient Detection of Copper(II) Ions. *Sens. Actuators B* **2014**, *190*, 516−522.
(12) Sun, Y. P.; Zhou, B.; Lin, Y.; Wang, W.; Fernando, K. A. S.; Pathak, P.; Meziani, M. J.; Harruff, B. A.; Wang, X.; Wang, H.; Luo, P. G.; Yang, H.; Kose, M. E.; Chen, B.; Veca, L. M.; Xie, S. Y. Quantum-Sized Carbon Dots for Bright and Colorful Photoluminescence. *J. Am. Chem. Soc.* **2006**, *128*, 7756−7757.
(13) Liu, M. L.; Chen, B.; Li, C. M.; Huang, C. Z. Carbon Dots: Synthesis, Formation Mechanism, Fluorescence Origin and Sensing Applications. *Green Chem.* **2019**, *21*, 449−471.
(14) Ding, H.; Yu, S.-B.; Wei, J.-S.; Xiong, H.-M. Full-Color Light-Emitting Carbon Dots with a Surface-State-Controlled Luminescence Mechanism. *ACS Nano* **2016**, *10*, 484−491.
(15) Song, Y.; Zhu, S.; Zhang, S.; Fu, Y.; Wang, L.; Zhao, X.; Yang, B. Investigation from Chemical Structure to Photoluminescent Mechanism: A Type of Carbon Dots from the Pyrolysis of Citric Acid and an Amine. *J. Mater. Chem. C* **2015**, *3*, 5976−5984.
(16) Bao, L.; Liu, C.; Zhang, Z.-L.; Pang, D.-W. Photoluminescence-Tunable Carbon Nanodots: Surface-State Energy-Gap Tuning. *Adv. Mater.* **2015**, *27*, 1663−1667.
(17) Wang, H.; Gao, P.; Wang, Y.; Guo, J.; Zhang, K. Q.; Du, D.; Dai, X.; Zou, G. Fluorescently Tuned Nitrogen-Doped Carbon Dots from Carbon Source with Different Content of Carboxyl Groups. *APL Mater.* **2015**, *3*, 1−8.
(18) Liu, W.; Li, C.; Ren, Y.; Sun, X.; Pan, W.; Li, Y.; Wang, J.; Wang, W. Carbon Dots: Surface Engineering and Applications. *J. Mater. Chem. B* **2016**, *4*, 5772−5788.
(19) Du, Y.; Guo, S. Chemically Doped Fluorescent Carbon and Graphene Quantum Dots for Bioimaging, Sensor Catalytic and Photoelectronic Applications. *Nanoscale* **2016**, *8*, 2532−2543.
(20) Kandasamy, G. Recent Advancements in Doped/Co-Doped Carbon Quantum Dots for Multi-Potential Applications. *J.Carbon Res.* **2019**, *5*, 24.
(21) Jiang, K.; Sun, S.; Zhang, L.; Lu, Y.; Wu, A.; Cai, C.; Lin, H. Red, Green, and Blue Luminescence by Carbon Dots: Full-Color Emission Tuning and Multicolor Cellular Imaging. *Angew. Chem. Int. Ed.* **2015**, *54*, 5360−5363.
(22) Qiao, Z. A.; Wang, Y.; Gao, Y.; Li, H.; Dai, T.; Liu, Y.; Huo, Q. Commercially Activated Carbon as the Source for Producing Multicolor Photoluminescent Carbon Dots by Chemical Oxidation. *Chem. Commun.* **2009**, *46*, 8812−8814.
(23) Wang, Y.; Hu, A. Carbon Quantum Dots: Synthesis, Properties and Applications. *J. Mater. Chem. C* **2014**, *2*, 6921−6939.
(24) Roy, P.; Chen, P. C.; Periasamy, A. P.; Chen, Y. N.; Chang, H. T. Photoluminescent Carbon Nanodots: Synthesis, Physicochemical Properties and Analytical Applications. *Mater. Today* **2015**, *18*, 447−458.
(25) Polis, B.; Samson, A. O. Role of the Metabolism of Branched-Chain Amino Acids in the Development of Alzheimer's Disease and Other Metabolic Disorders. *Neural Regen. Res.* **2020**, *15*, 1460−1470.
(26) Kale, A.; Kale, E. The Role of Amino Acids in Spina Bifida. *Clin. Exp. Obstet. Gynecol.* **2012**, *39*, 374−375.
(27) Levy, H. L.; Barkin, E. Comparison of Amino Acid Concentrations between Plasma and Erythrocytes. Studies in Normal Human Subjects and Those with Metabolic Disorders. *J. Lab. Clin. Med.* **1971**, *78*, 517−523.
(28) Zhou, Y.; Yoon, J. Recent Progress in Fluorescent and Colorimetric Chemosensors for Detection Ofamino Acids. *Chem. Soc. Rev.* **2012**, *41*, 52−67.
(29) Gao, Y.; Gao, F.; Zhang, G.; Chen, L.; Wu, Q.; Liu, X. Sensor Array Based on Single Carbon Quantum Dot for Fluorometric Differentiation of All Natural Amino Acids. *Microchim. Acta* **2019**, *186*, 858.
(30) Staros, J. V.; Wright, R. W.; Swingle, D. M. Enhancement by N-Hydroxysulfosuccinimide of Water-Soluble Carbodiimide-Mediated Coupling Reactions. *Anal. Biochem.* **1986**, *156*, 220−222.
(31) Lin, H.; Huang, J.; Ding, L. Preparation of Carbon Dots with High-Fluorescence Quantum Yield and Their Application in Dopamine Fluorescence Probe and Cellular Imaging. *J. Nanomater.* **2019**, *2019*, 1.
(32) Auld, D. S.; Holmquist, B.; Carboxypeptidase, A. Differences in the Mechanisms of Ester and Peptide Hydrolysis. *Biochemistry* **1974**, *13*, 4355−4361.
(33) Sahota, A.; Tischfield, J. A.; Goldfarb, D. S.; Ward, M. D.; Hu, L. Cystinuria: Genetic Aspects, Mouse Models, and a New Approach to Therapy. *Urolithiasis* **2019**, *47*, 57−66.
(34) Spodenkiewicz, M.; Spodenkiewicz, M.; Cleary, M.; Massier, M.; Fitsialos, G.; Cottin, V.; Jouret, G.; Poirsier, C.; Doco-Fenzy, M.; Lèbre, A. S. Clinical Genetics of Prolidase Deficiency: An Updated Review. *Biology. MDPI AG May* **2020**, *9*, 108.
(35) Sherman, K. E. Alanine Aminotransferase in Clinical Practice: A Review. *Arch. Intern. Med.* **1991**, *151*, 260.
(36) Harshman, R. A. Foundations of the PARAFAC Procedure: Models and Conditions for an "Explanatory" Multimodal Factor Analysis. *UCLA Working Paper.Phon.* **1970**, *16*, 1−84.
(37) Razavi, M.; Kompany-Zareh, M.; Khoshkam, M. PARAFAC Study of L-Cys@CdTe QDs Interaction to BSA, Cytochrome c and Trypsin: An Approach through Electrostatic and Covalent Bonds. *Spectrochim. Acta, Part A* **2021**, *246*, No. 119016.
(38) Cohen, J. E.; Bro, R. Nonnegative PARAFAC2: A Flexible Coupling Approach. *In Lecture Notes in Computer Science (including subseries Lecture Notes in Artificial Intelligence and Lecture Notes in Bioinformatics)*; Springer Verlag, 2018; Vol. *10891* LNCS, 89−98.
(39) Bro, R. PARAFAC. Tutorial and Applications. *Chemom. Intel. Lab. Syst.* **1997**, *38*, 149−171.

https://doi.org/10.1021/acsanm.1c01046
ACS Appl. Nano Mater. XXXX, XXX, XXX−XXX